Electronic Supplementary Material (ESI) for Catalysis Science & Technology.
This journal is © The Royal Society of Chemistry 2024

Electronic Supplementary Information

Highly active and stable RuO_2/MgF_2 catalysts for efficient HCl oxidation in the fluorochemical industry

Yufeng Gong[†,a], Siheng Nie [†,a], Honglin Ji [a], Linying Fu [a], Rui Ma[a,b,*], Xinqing Lu[a,b], Yanghe Fu[a,b], Weidong Zhu[a,b,c,*]

[a] *Zhejiang Engineering Laboratory for Green Syntheses and Applications of Fluorine-Containing Specialty Chemicals, Institute of Advanced Fluorine-Containing Materials, Zhejiang Normal University, 321004 Jinhua, People's Republic of China*

[b] *Key Laboratory of the Ministry of Education for Advanced Catalysis Materials, Institute of Physical Chemistry, Zhejiang Normal University, 321004 Jinhua, People's Republic of China*

[c] *National Engineering Technology Research Center of Fluoro-Materials, Zhejiang Juhua Technology Center Co., Ltd., 324004 Quzhou, People's Republic of China*

[†]These authors contributed equally to this work.

*To whom correspondence should be addressed.

Tel./Fax: +86 579 82282234; E-mail: mr@zjnu.cn (R. Ma);

Tel./Fax: +86 579 82282932; E-mail: weidongzhu@zjnu.cn (W. Zhu)

Models for the kinetic adsorption of Ru ions on MgF_2-SRT supports

Evaluation on mass transfer limitations

Fig. S9. XRD pattern of the used RuO_2/MgF_2-1 catalyst.

Fig. S10. TEM (C) and HRTEM (D) images of the used RuO_2/MgF_2-1 catalyst.

Fig. S11. Raman spectrum of the used RuO_2/MgF_2-1 catalyst.

Fig. S12. Ru 3d (A) and Cl 2p (B) XPS spectra of the used RuO_2/MgF_2-1 catalyst.

Models for the kinetic adsorption of Ru ions on MgF_2-SRT supports

To quantitatively analyze the adsorption kinetics of Ru ions on MgF_2-SRT supports, the plots of q_t versus t were further analyzed by employing the pseudo first-order and pseudo second-order models as shown in Equations (S1) and (S2) [1].

Pseudo first-order model:

$$\ln (q_e - q_t) = \ln q_e - k_1 t \qquad \text{(S1)}$$

Pseudo second-order model:

$$\frac{t}{q_t} = \frac{1}{k_2 q_e^2} + \frac{t}{q_t} \qquad \text{(S2)}$$

where q_t and q_e in $\mu mol \cdot g^{-1}$ are the adsorption amounts of Ru ions at time t and equilibrium, respectively, t represents the contact time (min), and k_1 (min^{-1}) and k_2 ($g \cdot \mu mol^{-1} \cdot min^{-1}$) are denoted as the rate constants for the above two models, respectively.

Reference

1. S. S. Gupta, K.G. Bhattacharyya, *Adv. Colloid Interface Sci.*, 2011, **162**, 39-58.

Evaluation on mass transfer limitations

The influence of mass transfer limitations on reaction kinetics was evaluated using the Mears (C_M) and Weisz-Prater (C_{WP}) criteria, which were calculated using Equations (S3) and (S4), respectively [1,2].

$$C_M = \frac{n \cdot r_{\text{obs}} \cdot \rho_{\text{cat}} \cdot R_{\text{cat}}}{k_c \cdot C_{\text{HCl}}} \quad \text{(S3)}$$

$$C_{WP} = \frac{r_{\text{obs}} \cdot \rho_{\text{cat}} \cdot R_{\text{cat}}^2}{D_{\text{eff}} \cdot C_{\text{HCl,s}}} \quad \text{(S4)}$$

where n is the reaction order, r_{obs} is the observed reaction rate, ρ_{cat} is the bulk density of catalyst bed, R_{cat} is the particle radius of catalyst, k_{c} is the external mass transfer coefficient, C_{HCl} is the bulk concentration of HCl, D_{eff} is the effective diffusion coefficient and $C_{\text{HCl,s}}$ is the HCl concentration on the surface of a catalyst particle, which is equal to C_{HCl} when the external mass transfer limitation is neglected.

k_{c} was estimated with Equations (S5)-(S7) by means of similarity numbers such as the Sherwood number Sh, the Reynolds number of the catalyst pellet Re_{p}, and the Schmidt number S_{c} [1].

$$Sh = \frac{k_{\text{c}} \cdot d_{\text{cat}}}{D_{\text{eff}}} = 2 + 0.6 \cdot Re_{\text{p}}^{1/2} \cdot Sc^{1/3} \quad \text{(S5)}$$

$$Re_{\text{p}} = \frac{U \cdot \rho \cdot d_{\text{cat}}}{\mu} \quad \text{(S6)}$$

$$Sc = \frac{\mu}{D_{\text{eff}} \cdot \rho} \quad \text{(S7)}$$

where d_{cat} is the diameter of a catalyst particle, U is the free-stream velocity, ρ and μ are the density and viscosity of a feed mixture, which can be determined from Aspen Plus software.

D_{eff} was estimated with Equations (S8)-(S11) using the coefficients for Knudsen

diffusion D_A^K and bulk diffusion D_A^b [1].

$$\frac{1}{D_{eff}} = \frac{1}{D_A^K} + \frac{1}{D_A^b} \quad \text{(S8)}$$

$$D_A^K = \frac{2}{3} \cdot r_{po} \cdot \sqrt{\frac{8 \cdot R \cdot T}{\pi \cdot M_i}} \cdot \frac{\varepsilon}{\tau} \quad \text{(S9)}$$

$$r_{po} = 4 \cdot \frac{\varepsilon}{S_{cat} \cdot \rho_{cat,g}} \quad \text{(S10)}$$

$$D_A^b = D_A \cdot \frac{\varepsilon}{\tau} \quad \text{(S11)}$$

where ε, τ, r_{po}, S_{cat}, and $\rho_{cat,g}$ are the porosity, tortuosity, average pore radius, surface area, and grain density of catalyst, T and M_i are the temperature and relative molecular weight of component i, and D_A is the free diffusion coefficient, which can be determined from Aspen Plus software.

The data used in the above-mentioned equations and the calculations of the Mears and Weisz-Prater parameters are given in Tables S3 and S4. Apparently, C_M/n is less than 0.15 while n ranges from 1 to 2, implying that there is no external mass-transfer limitation. In addition, C_{WP} is much less than 1 at different temperatures, indicating that the internal diffusion limitations can be neglected.

References:

1. H. S. Fogler, *Diffusion and reaction in elements of chemical reaction engineering*, Pearson Education Inc.: New York, 2016, pp 734-743.

2. T. R. Marrero, E.A. Mason, *J. Phys. Chem. Ref. Data*, 1972, **1**, 1-118.

Table S1. Extracted parameter values for the kinetic adsorption of Ru ions on MgF_2-SRT supports at 30.0 °C

Support	Pseudo first-order parameters			Pseudo second-order parameters		
	q_e (μmol·g^{-1})	k_1 (min^{-1})	R^2	q_e (μmol·g^{-1})	k_2 (g·μmol^{-1}·min^{-1})	R^2
MgF_2-1	117	0.51	0.834	120	0.63	0.993
MgF_2-8	101	0.43	0.786	104	0.52	0.996
MgF_2-24	75	0.38	0.802	77	0.41	0.995
MgF_2-36	56	0.32	0.819	58	0.34	0.995

Table S2. Measured reaction rates over RuO_2/MgF_2-SRT catalysts at different reaction temperatures for E_a calculations[a]

Catalyst	Temperature (°C)	HCl conversion (%)	Reaction rate ($\times 10^{-4}$ mol·g^{-1}·s^{-1})
RuO_2/MgF_2-1	305	1.58	7.9
	315	1.86	9.3
	325	1.96	9.8
	335	2.28	11.4
	345	2.71	13.6
	355	3.62	18.1
RuO_2/MgF_2-8	305	1.27	6.4
	315	1.48	7.4
	325	1.79	9.0
	335	2.10	10.5
	345	2.47	12.4
	355	3.10	15.5
RuO_2/MgF_2-24	305	0.94	4.7
	315	1.13	5.7
	325	1.45	7.3
	335	1.69	8.5
	345	1.94	9.7

	355	2.24	11.2
RuO_2/MgF_2-36	305	0.84	4.2
	315	1.03	5.2
	325	1.16	5.8
	335	1.29	6.5
	345	1.49	7.5
	355	1.77	8.9

[a] The different, high gas hourly space velocities were set in order to maintain HCl conversions always below 10%, and the reaction rates were measured after 1 h of the oxidation reaction.

Table S3. Data for calculating the Mears and Weisz-Prater criterion parameters

Parameters	Values
ρ_{cat}	806 kg·m^{-3}
R_{cat}	0.20 mm
$\rho_{cat,g}$	3,074 kg·m^{-3}
ε	0.65
τ[a]	3

[a] The pore tortuosity was assumed to be 3 for a spherical catalyst particle.

Table S4. Evaluation on the Mears (C_M) and Weisz-Prater (C_{WP}) criterion parameters

Catalyst	Temperature (°C)	C_M	C_{WP}
RuO_2/MgF_2-1	325	4.5×10^{-3}	1.8×10^{-2}
	335	5.5×10^{-3}	2.2×10^{-2}
	345	6.9×10^{-3}	2.7×10^{-2}
	355	8.9×10^{-3}	3.5×10^{-2}
RuO_2/MgF_2-8	325	5.6×10^{-3}	2.2×10^{-2}
	335	6.5×10^{-3}	2.6×10^{-2}
	345	7.5×10^{-3}	3.0×10^{-2}
	355	8.8×10^{-3}	3.5×10^{-2}
RuO_2/MgF_2-24	325	7.4×10^{-3}	3.1×10^{-2}
	335	8.6×10^{-3}	3.6×10^{-2}
	345	9.9×10^{-3}	4.1×10^{-2}
	355	1.1×10^{-2}	4.7×10^{-2}
RuO_2/MgF_2-36	325	5.8×10^{-3}	2.4×10^{-2}
	335	6.7×10^{-3}	2.7×10^{-2}
	345	8.1×10^{-3}	3.3×10^{-2}
	355	9.7×10^{-3}	3.9×10^{-2}

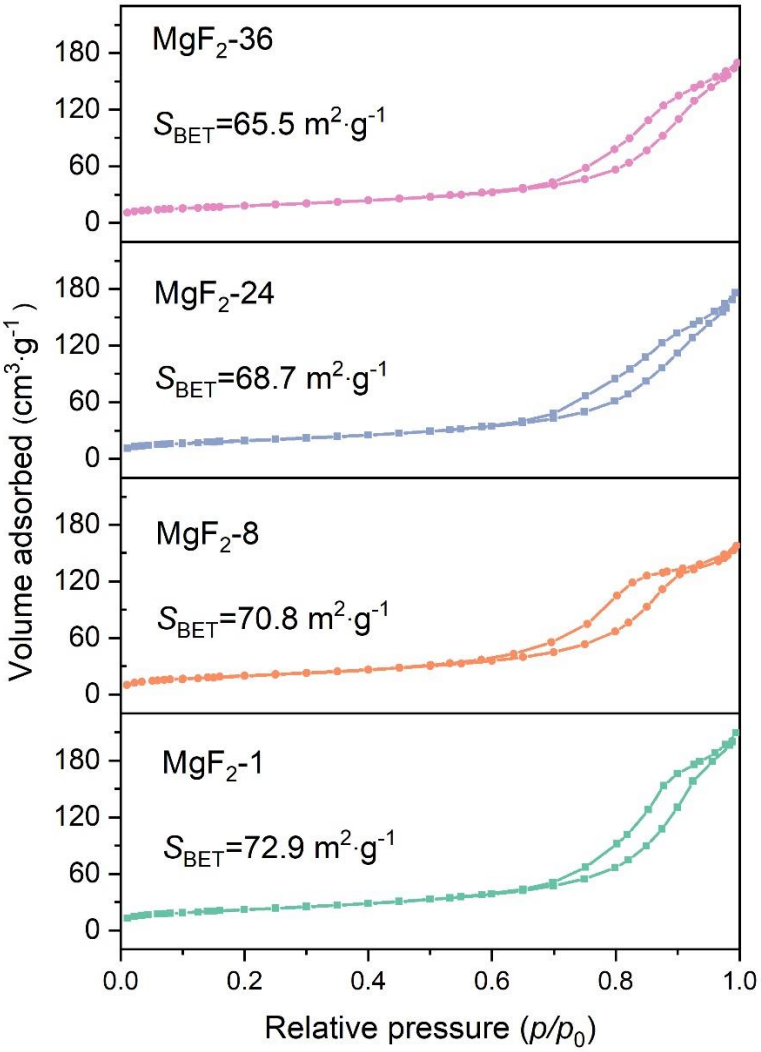

Fig. S1. Adsorption-desorption isotherms of N_2 on MgF_2-SRT supports at -196.0 ºC.

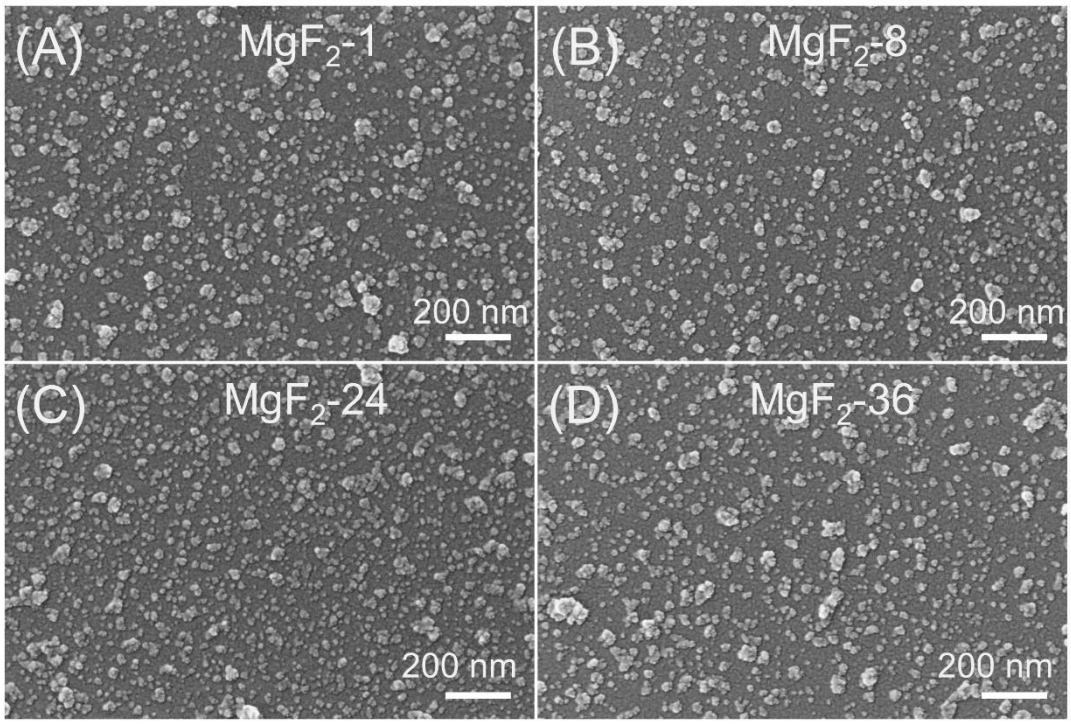

Fig. S2. SEM images of MgF_2-SRT supports.

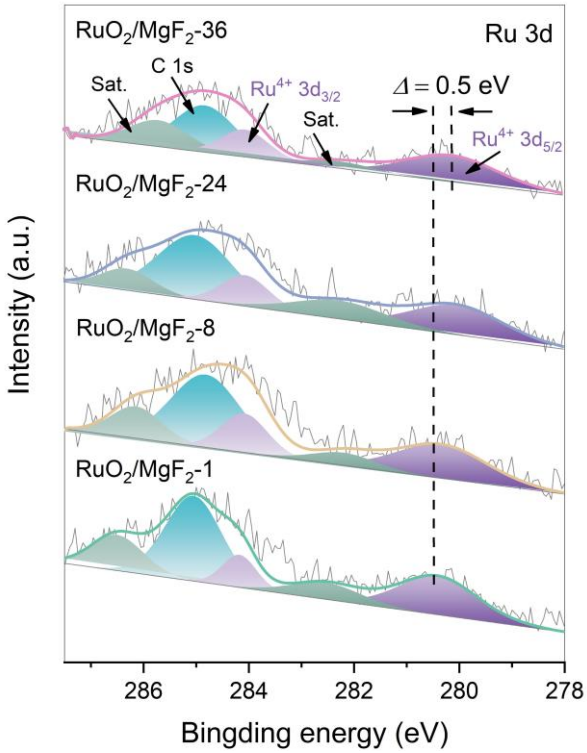

Fig. S3. Ru 3d XPS spectra of RuO_2/MgF_2-SRT catalysts.

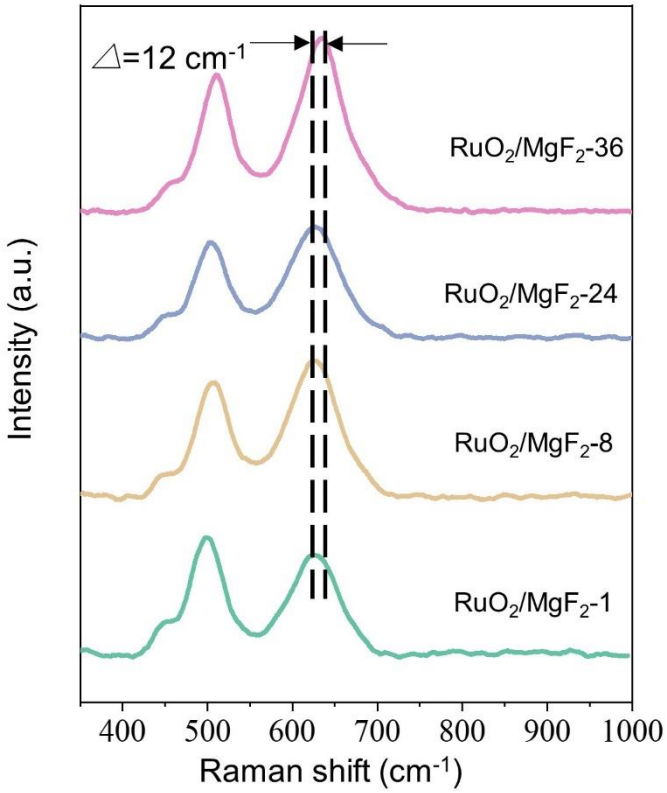

Fig. S4. Raman spectra of RuO_2/MgF_2-SRT catalysts.

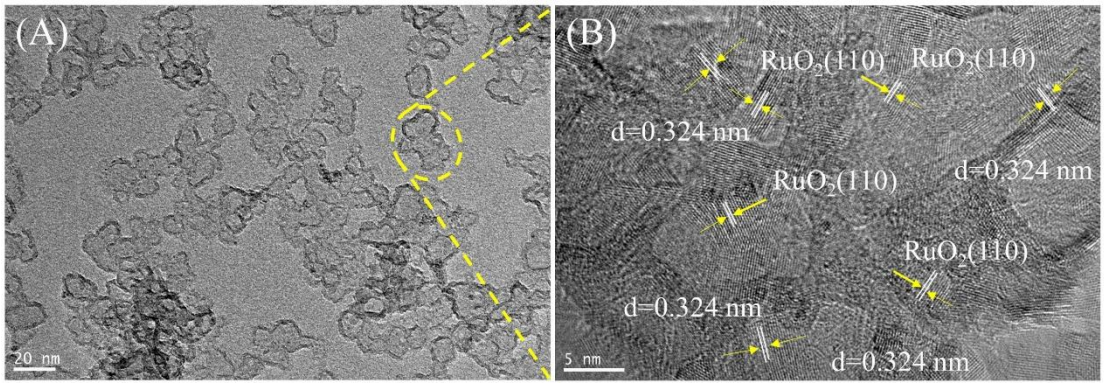

Fig. S5. TEM (A) and HRTEM (B) images of RuO_2/MgF_2-1 catalyst.

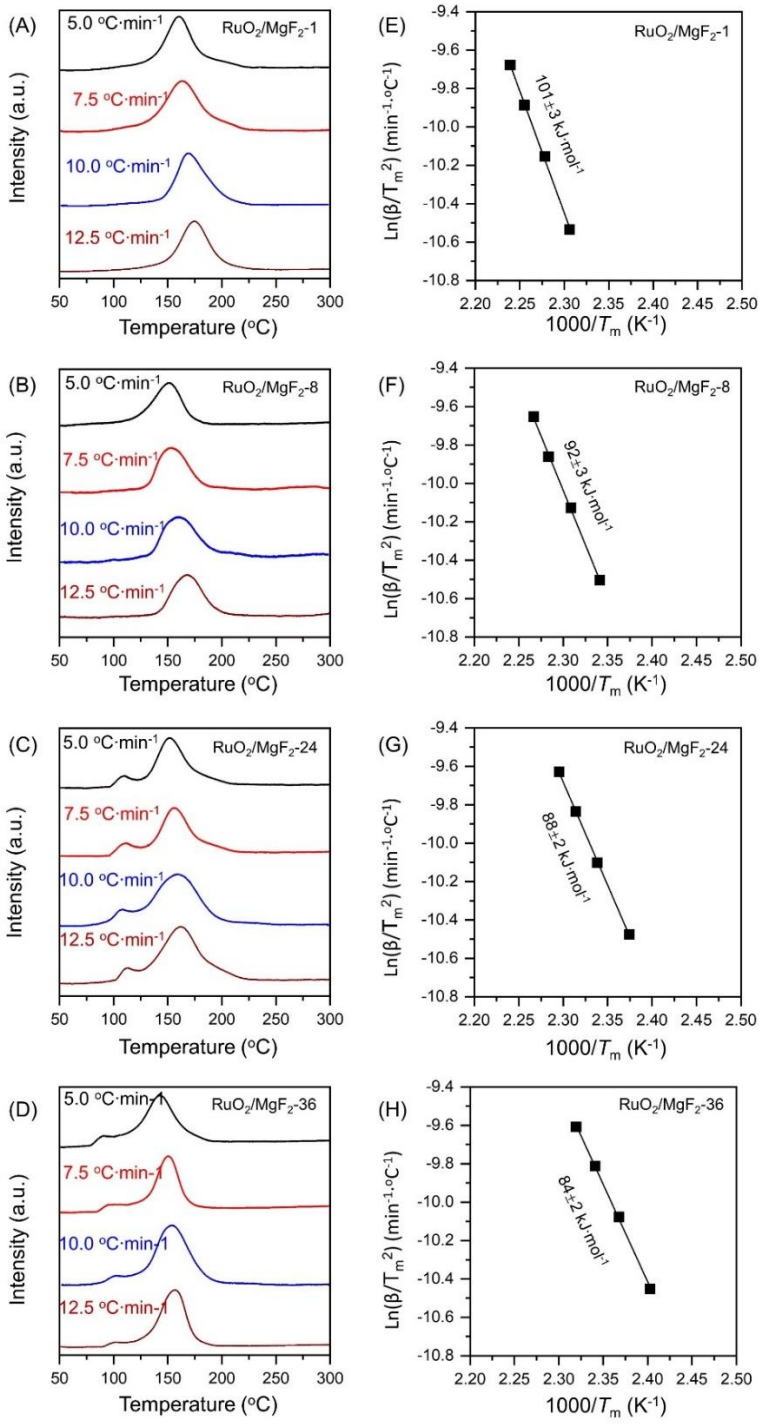

Fig. S6. H_2-TPR curves at different heating rates for RuO_2/MgF_2-SRT catalysts and the Kissinger plots for the reduction peaks of RuO_2/MgF_2-SRT catalysts. The apparent activation energy of the Ru-O bond dissociation was calculated by the Kissinger equation.

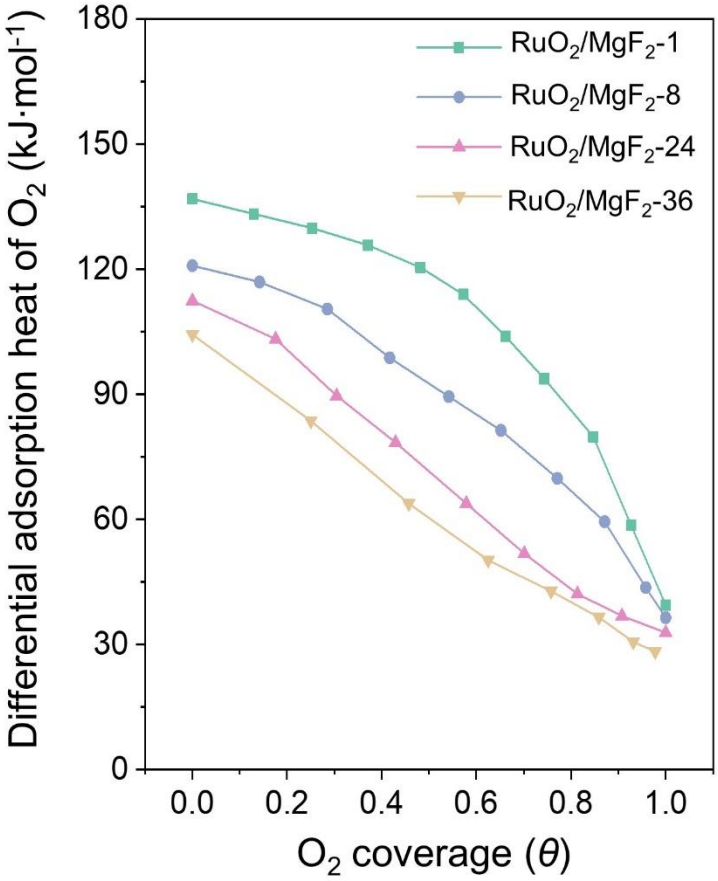

Fig. S7. Differential adsorption heat of O_2 on RuO_2/MgF_2-SRT as a function of O_2 coverage (θ) at 40.0 °C.

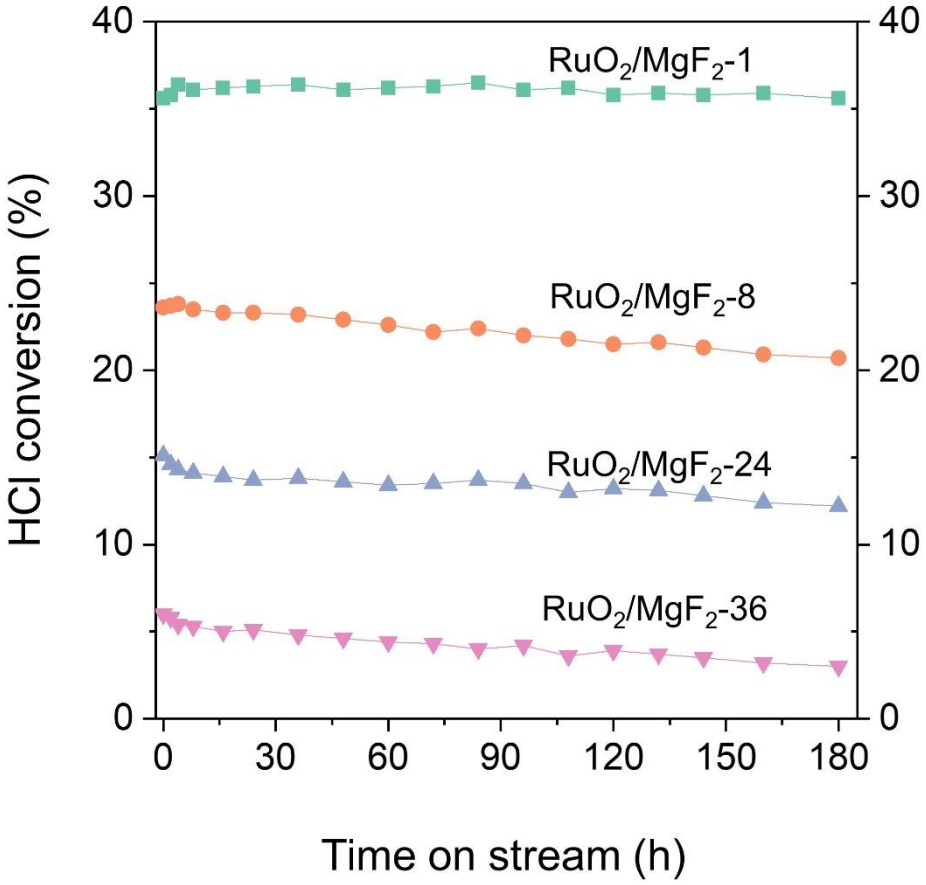

Fig. S8. HCl conversion as a function of time on stream over RuO_2/MgF_2-SRT catalysts. Reaction conditions: 350 ºC and a GHSV of 48,000.0 mL (STP)·$(h \cdot g_{catal})^{-1}$.

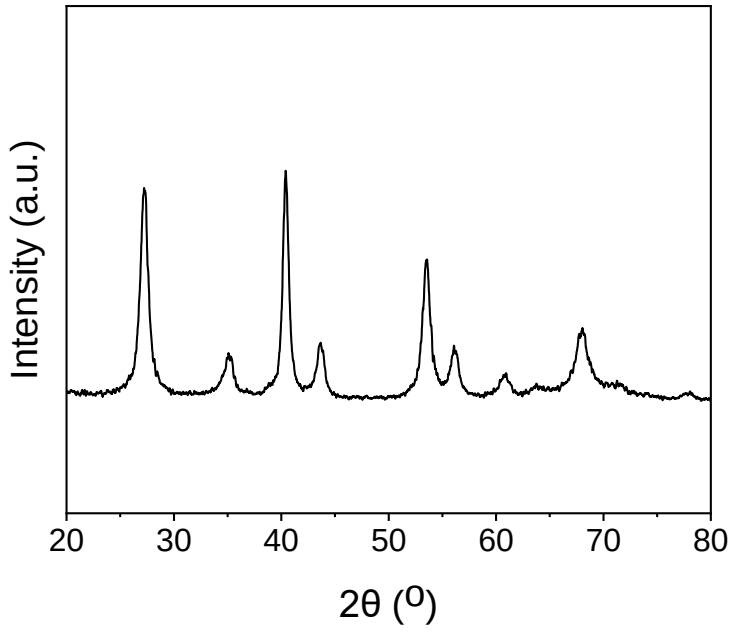

Fig. S9. XRD pattern of the used RuO_2/MgF_2-1 catalyst.

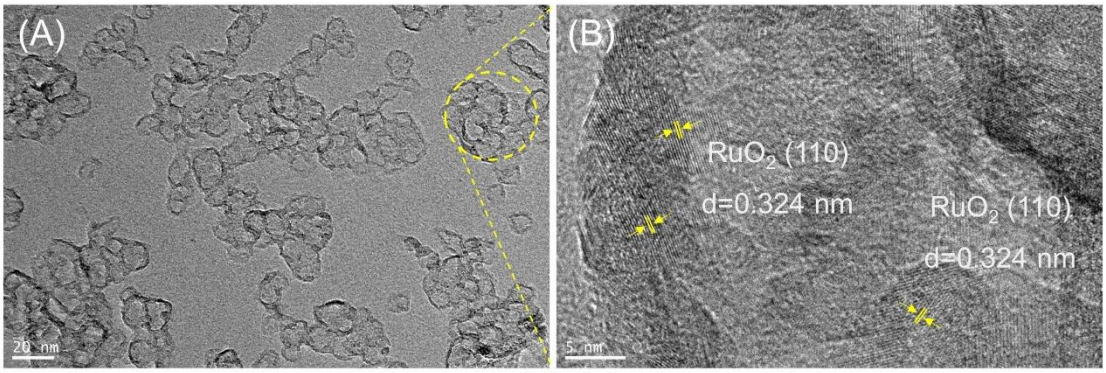

Fig. S10. TEM (A) and HRTEM (B) images of the used RuO_2/MgF_2-1 catalyst.

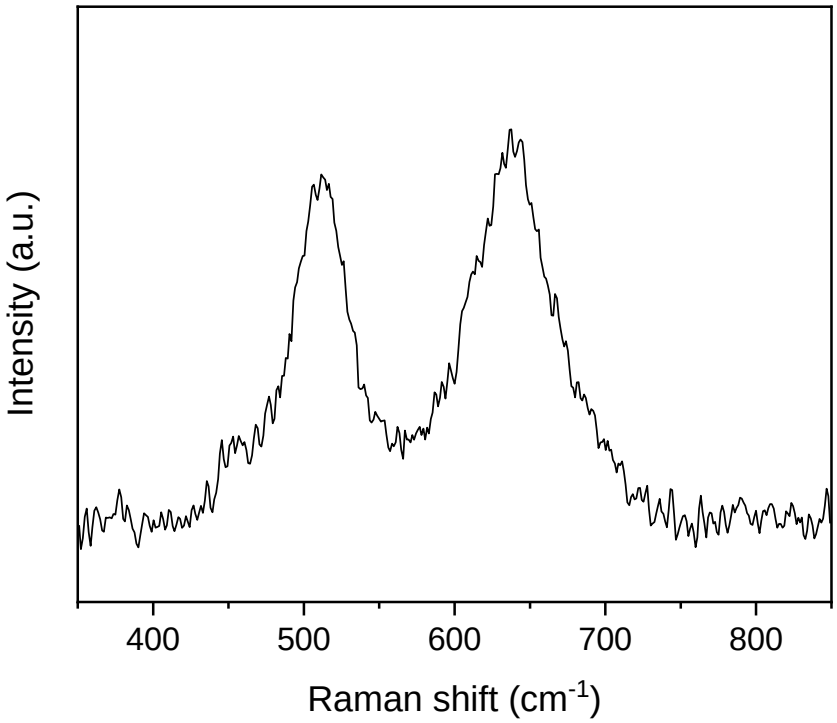

Fig. S11. Raman spectrum of the used RuO_2/MgF_2-1 catalyst.

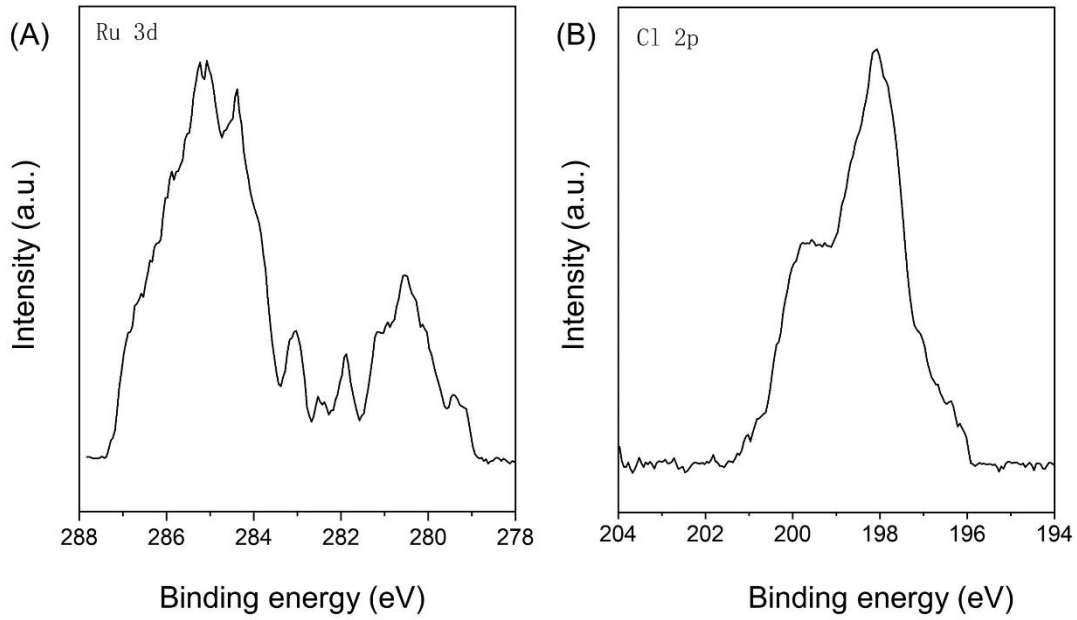

Fig. S12. Ru 3d (A) and Cl 2p (B) XPS spectra of the used RuO_2/MgF_2-1 catalyst.